

Triangular *in Vivo* Self-Assembling Coiled-Coil Protein OrigamiSabina Božič Abram,[▽] Helena Gradišar,[▽] Jana Aupič, Adam R. Round, and Roman Jerala*^{*}Cite This: *ACS Chem. Biol.* 2021, 16, 310–315

Read Online

ACCESS |



Metrics & More

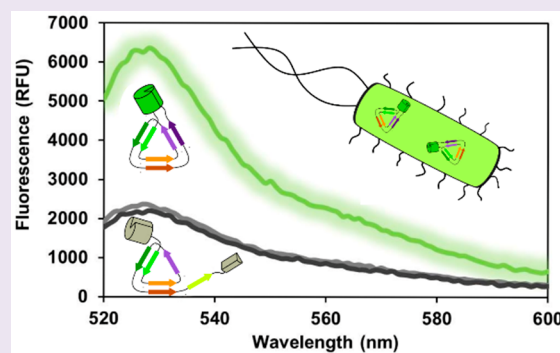


Article Recommendations



Supporting Information

ABSTRACT: Coiled-coil protein origami (CCPO) polyhedra are designed self-assembling nanostructures constructed from coiled coil (CC)-forming modules connected into a single chain. For testing new CCPO building modules, simpler polyhedra could be used that should maintain most features relevant to larger scaffolds. We show the design and characterization of nanoscale single-chain triangles, composed of six concatenated parallel CC dimer-forming segments connected by flexible linker peptides. The polypeptides self-assembled in bacteria in agreement with the design, and the shape of the polypeptides was confirmed with small-angle X-ray scattering. Fusion with split-fluorescent protein domains was used as a functional assay in bacteria, based on the discrimination between the correctly folded and misfolded nanoscale triangles comprising correct, mismatched, or truncated modules. This strategy was used to evaluate the optimal size of linkers between CC segments which comprised eight amino acid residues.



For the large majority of structural and functional tasks in cells, proteins are nature's material of choice. Nevertheless, nucleic acids have been repurposed for the assembly of designed bionanostructures that exploit the pairwise complementarity between strands of nucleic acids.^{1–3} The relationship between sequence and structure is straightforward for the DNA duplex, whereas predicting polypeptide interactions remains more challenging. However, compared to DNA, polypeptides as the nanostructure building material offer greater structural and functional diversity, because they are composed of 20 amino acids with different chemical properties. In addition, proteins can be produced cost-effectively on a large scale using biotechnological methods, which make proteins attractive for designed bionanomaterials.⁴ Several strategies have been developed for the design of new protein structures based on techniques such as directed evolution,^{5,6} introduction of interaction surfaces on natural oligomerization domains,^{7–9} fusion of oligomerization domains with matching symmetries,^{10–13} and assembly of secondary structure modules.^{14–18} A coiled-coil (CC) dimer is an appealing building module for *de novo* polypeptide nanostructures. Arguably, α -helical coiled coil is the best-understood supersecondary structure module.¹⁹ It is defined by its oligomerization state, orientation, stability, and partner specificity.²⁰ Several nanoassemblies have been constructed from concatenated CC-forming peptides^{14,21,22} from multiple copies of two or more different polypeptide chains. Recently, an approach was introduced for the self-assembly of modular designed protein nanostructures, which does not rely on the symmetric assembly of natural protein domains but on the precisely defined topological path of the polypeptide chain that

interlocks the interacting CC segments into a defined shape.²³ A single polypeptide chain, comprising concatenated CC-forming segments connected by flexible peptide linkers, threads the chain into the designed shape, such as a nanoscale tetrahedron, in which the polypeptide chain traverses each edge twice; therefore CC dimeric segments form its edges while linkers are positioned in the vertices of the polyhedra. The sequential order of CC building modules uniquely defines the path where scrambling of their order results in misfolded structures. We proposed the term topofolds or coiled-coil protein origami (CCPO) for structures designed according to this strategy.²⁴ The number of possible topological solutions for each polyhedral fold increases with the increasing number of edges and typically requires the use of parallel and antiparallel CC dimers. A strategy for the rapid prototyping of the building blocks suitable for the construction of designed modular protein polyhedra would enable faster and more reliable design. Although characterization of each isolated CC-forming peptide pair regarding its specificity and stability provides some information about the pair's suitability as a building module, analysis within the context of a polyhedron would provide much more valuable information. A single-chain design introduces high local concentration of CC-forming segments, which might enable formation of CC dimers even

Received: October 13, 2020

Accepted: December 14, 2020

Published: January 21, 2021



for weakly interacting modules. Additionally, preorganization of the partially folded structure positions the interaction segments into close proximity, introducing some degree of cooperativity. Additionally testing different linker peptides requires the appropriate context. Therefore, there is no better substitute for evaluating different linker or edge-forming modules than within the prototyping polyhedra. We decided to investigate the design of nanotriangles as the prototyping single-chain polyhedron and their potential for screening CCPO building modules. We show that polypeptide triangles fold into a desired shape and enable the analysis of the effect of different building modules using split-fluorescent protein strategy.

RESULTS AND DISCUSSION

Design of Single-Chain Triangular Polypeptides.

Aiming to design a single-chain polypeptide triangle as a prototyping fold, we realized that the polypeptide chain for the triangular fold could be composed of three orthogonal coiled coil (CC)-forming segments followed by three counterpart pairing segments. Three orthogonal parallel heterodimeric CC pairs PmS:PnS (P3S:P4S, P5S:P6S, and P7S:P8S, sequences in Supporting Information Table 1) were selected from a set of four-heptad coiled coils, previously designed *de novo*²⁵ and modified at positions *b*, *c*, and *f* in heptad repeats to increase their solubility.^{20,26} In the triangle-forming design TRI6, the CC-forming modules are connected in the following order: P3S–P7S–P5S–P4S–P8S–P6S (Figure 1a).

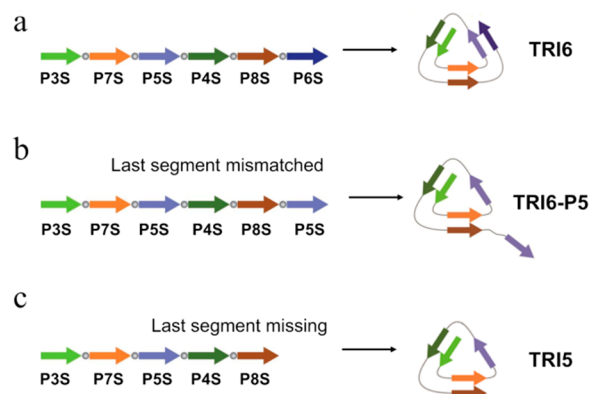


Figure 1. Schematic representation of designed polypeptides to fold into triangular structures with controls. (a) The polypeptide TRI6 self-assembles into a regular triangle. Two negative controls, TRI6-P5 with a mismatched last segment (b) and TRI5 lacking a C-terminal coiled coil-forming segment (c), form irregular triangles. Circles in polypeptide chains represent the (SG)₄ peptide linker. Arrows denote the orientation of the interacting peptide segments in the assembly. The amino acid sequences are presented in Supporting Information Table 2.

The flexible linkers between the coiled-coil-forming segments disrupt the continuity of the helices and permit an acute angle between the edges. It has been shown previously on a multiple chain design that the length of a polypeptide linker can determine whether a discrete closed architecture or linear oligomers are formed.^{21,27} For our initial design, four repeats of the dipeptide Ser–Gly ((SG)₄) were used to ensure flexibility and helix termination between the CC segments of TRI6. Two negative controls were designed, which should not be able to form a triangular fold with the coinciding polypeptide N- and

C-chain termini. In the first control design TRI6-P5, the C-terminal segment P6S which closes the triangle TRI6 was replaced by a second repeat of the segment P5S (Figure 1b). This control with a mismatched C-terminal segment should not form a stable triangular fold because a homodimeric pair P5S–P5S is disfavored by two Asn–Ile mismatches and charge repulsion. In such a design, we can expect the formation of two of the three coiled-coil segments and correspondingly different helical content of the formed structure. An additional design, with a similar anticipated effect, however, without the possibility of a coiled-coil segment mismatch is the polypeptide TRI5 that lacks the C-terminal segment P6S (Figure 1c). In this design, the segment P5S is expected to remain unpaired and unstructured.

Production and Characterization of Triangular Polypeptides. Polypeptides TRI6, TRI6-P5, and TRI5 were expressed in *Escherichia coli* based on the introduction of synthetic genes and isolated under the native conditions from the soluble fractions of lysed cells (Supporting Information Figure 1a). Purified proteins were analyzed by circular dichroism to determine the secondary structure content. The helical content was the highest at 73% for the designed nanotriangle TRI6 and lower for both negative controls (Figure 2a); the helical content of TRI6-P5 was slightly higher (49%) than that of TRI5 (43%). Thermal stability measurement (Figure 2b) demonstrated that TRI6 and TRI5 exhibit a two-state unfolding profile, with the presence of additional states apparent at a lower temperature for TRI6-P5. Most likely, the additional transition at a lower temperature may be

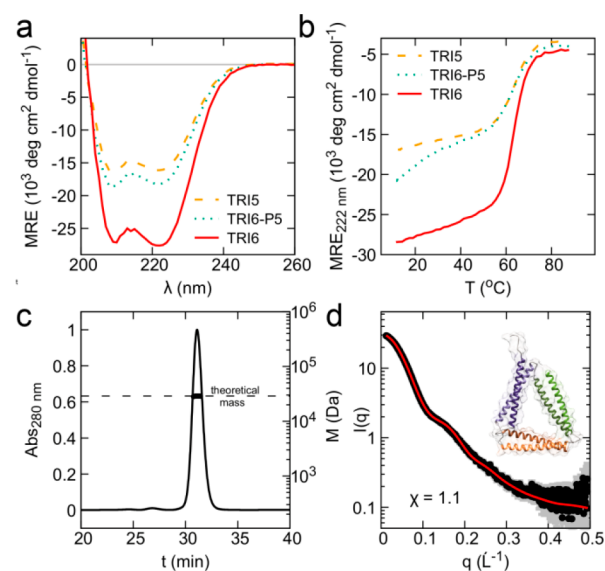


Figure 2. Biophysical and structural characterization of isolated polypeptide particles. (a) Analysis of the secondary structure for the polypeptides TRI6, TRI6-P5, and TRI5, performed by circular dichroism measurements. Each curve represents the average of three scans. (b) Thermal denaturation curves of the polypeptides TRI6, TRI6-P5, and TRI5 obtained by measuring circular ellipticity at 222 nm in the temperature range from 10 to 90 °C. (c) SEC-MALS confirmed the monomeric state and highly uniform TRI6 particles. (d) Comparison of the experimental SAXS profile of TRI6 (black dots) with the theoretical scattering profile of the best-fitting molecular model (red line). Experimental error is shown in gray. (Inset) The TRI6 model structure that best describes the observed SAXS data.

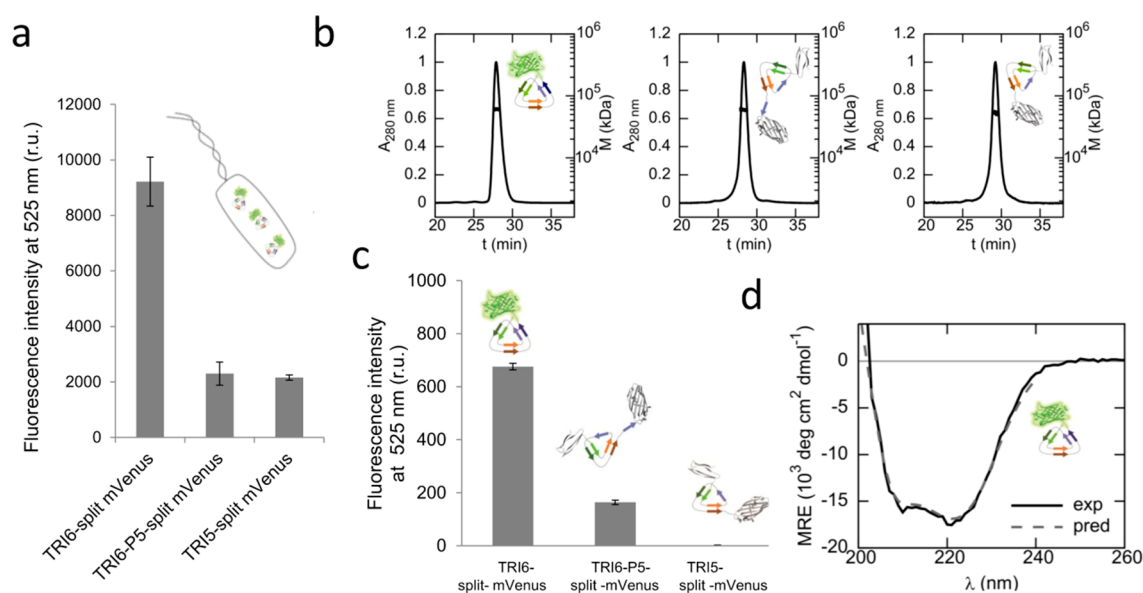


Figure 3. Detection of the correctly folded polypeptide polyhedra based on *in vivo* and *in vitro* fluorescence reconstitution. (a) Relative fluorescence intensity of bacterial cell suspensions expressing TRI6^{split-mVenus}, TRI6-P5^{split-mVenus}, and TRI5^{split-mVenus} was measured. Data are the means of three independent samples. (b) The isolated polypeptides fused with the split fluorescent protein were characterized by SEC-MALS (left, TRI6^{split-mVenus}; middle, TRI6-P5^{split-mVenus}; right, TRI5^{split-mVenus}). (c) Relative fluorescence intensity of isolated polypeptides was determined at 525 nm using excitation at 495 nm. (d) CD measurement for TRI6^{split-mVenus}. The experimental curve that represents the average of three scans is compared to the predicted signal.

due to the weak interactions between the two PSS segments in TRI6-P5. Although the PSS peptide does not form homodimers at the 20 μ M concentration,²⁰ the peptide may weakly homodimerize in the triangular structure due to the high local concentration imposed by the preorganized structure and, therefore, slightly increase the helical content of TRI6-P5. According to the design of TRI6, the coiled-coil-forming segments must dimerize intramolecularly to fold into a proper triangular structure. To confirm the formation of the coiled-coil dimers within a single chain and not through the association of two or multiple polypeptide chains, the oligomeric state of all polypeptide triangles was determined by size-exclusion chromatography coupled with multiangle light scattering (SEC-MALS) measurement (Figure 2c, Supporting Information Figure 2a). The isolated polypeptide TRI6 was monodispersed with 98% homogeneity, while chromatograms of negative controls TRI6-P5 and TRI5 revealed a small fraction of oligomers (Supporting Information Figure 2b,c).

The molecular mass of TRI6 calculated from the experimental data is 28.8 ± 0.1 kDa, which is in agreement with the calculated molecular mass of 28.8 kDa, suggesting that TRI6 is monomeric. The TRI6 particles were further structurally characterized by SAXS measurements (Figure 2d, Supporting Information Figure 3). Guinier analysis of the scattering intensities at low values of the scattering vector led to an R_g of $2.9 \text{ nm} \pm 0.1 \text{ nm}$ and to a molecular mass estimated from $I(0)$ of $30.2 \text{ kDa} \pm 0.2 \text{ kDa}$. Additionally, the experimental scattering profile was compared to the atomistic models of TRI6 created with the CoCoPOD platform.²⁴ To account for conformational heterogeneity, we built 30 model structures, however all were fairly similar most likely due to the small size of the designed assembly (Supporting Information Figure 4). We obtained good agreement with several models; the best model had a χ value of 1.1, corroborating that TRI6 assumes the designed triangular shape in solution.

Triangular Polypeptides with Split-Fluorescent Protein Domains. The proximity of the N- and C-termini of the polypeptide chain in CCPO polyhedra could be detected by a bimolecular fluorescence complementation.²³ The fluorescence of a split fluorescent protein is reconstituted only when the polypeptide folds according to the design and the termini of a chain come in the proximity at the same vertex (TRI6). In the case of a negative control TRI5, the distance between the subdomains should prevent reconstitution of the fluorescent protein. Additionally, the design of the variant TRI6-P5 provided the control to investigate whether a nonstructured segment between the split fluorescent protein domains at the termini might nevertheless allow reconstitution of the fluorescent protein domain. Therefore, subdomains of split mVenus (sequence in Supporting Information Table 3) were fused to the N- and C-termini of the polypeptide TRI6 and negative controls TRI6-P5 and TRI5, to test the system's ability to discriminate between the polypeptide folds with and without coinciding termini. The corresponding fusion proteins were named TRI6^{split-mVenus}, TRI6-P5^{split-mVenus}, and TRI5^{split-mVenus} (Supporting Information Figure 5; amino acid sequences in Supporting Information Table 2).

***In Vivo* and *In Vitro* Fluorescence Reconstitution.** All proteins were expressed in *E. coli*, and the fluorescence of the bacterial cell suspension was measured 4 h after the induction at 30 °C. Results show that the *in vivo* fluorescence levels for both negative controls TRI6-P5^{split-mVenus} and TRI5^{split-mVenus} were significantly lower than that of TRI6^{split-mVenus} (Figure 3a).

The platform for the design of split reporter nanotriangles should be able to detect the fluorescence reconstitution that occurs as a result of the proximity between the N- and C-termini within the folded single polypeptide chain. However, fluorescence might, in principle, also be reconstituted by the assembly from multiple polypeptide chains. Therefore, we isolated all polypeptides (TRI6^{split-mVenus}, TRI6-P5^{split-mVenus}, and TRI5^{split-mVenus}) under the native conditions. The purity of

the isolated polypeptides was confirmed by SDS-PAGE (Supporting Information Figure 1b), and monodispersity was checked by SEC-MALS (Figure 3b). From the comparison of the chromatograms, it is evident that all proteins, TRI6^{split-mVenus} and both negative controls, are isolated as monomeric. For TRI6^{split-mVenus}, 97% of the protein corresponded to the molecular mass of 60.9 kDa \pm 0.6, which matches well to the theoretically calculated molecular mass of 55.1 kDa, respectively. In addition, the ratio between the fluorescence intensity of TRI6^{split-mVenus} is at least 4-times higher in comparison to controls TRI6-P5^{split-mVenus} and TRI5^{split-mVenus} (Figure 3c). Circular dichroism measurement showed that TRI6^{split-mVenus} is comprised of 40% α -helix and 18% β -sheet, which is consistent with the predicted secondary structure content from the molecular model (Figure 3d).

The Effect of Length of Linker between Concatenated Segments. After confirming the suitability of the proposed method for detecting correctly matched CC segments, we further tested whether this platform is suitable for discerning more subtle differences in the design, such as the linker length between concatenated peptide segments, which could not be inferred from experiments on CC peptides. Four additional variants of the polypeptide TRI6 were prepared with varied linker lengths, fused to the split mVenus domains at the N- and C-termini. The fluorescence of bacteria expressing a polypeptide without linker (TRI6-(SG)₀^{split-mVenus}) was compared to the fluorescence of cells expressing polypeptides with a four (TRI6-(SG)₂^{split-mVenus}), six (TRI6-(SG)₃^{split-mVenus}), or eight (TRI6-(SG)₄^{split-mVenus}) amino acid linker. Results show the highest relative fluorescence for polypeptides with six or eight residue linkers (Figure 4a), which seem to be required for

the formation of an acute angle in a triangular structure similar to the requirement of the length of loop regions in DNA-based polyhedra.²⁸ A strong decrease in the fluorescent signal was observed in cells expressing a designed variant without a linker. Similar results were also obtained upon measuring the *in vitro* fluorescence of isolated polypeptides (Figure 4b, Supporting Information Figure 1c), confirming the suitability of the system to evaluate the effect of different building blocks directly in bacterial cells.

Assemblies of triangles and rectangles have been previously demonstrated using multiple coiled-coil-forming peptides.^{21,27} In those cases, the assemblies were composed of multiple chains and the equilibrium assembly depended on the concentration. The advantage of the single-polypeptide chain platform is that it leads to a highly monodisperse assembly that is independent of the concentration with low conformational heterogeneity. Closed two-dimensional architectures from peptides composed of two complementary coiled-coil-forming segments were previously used to elucidate the influence of steric constraints imposed on the geometry of the assemblies by linker regions.²¹ Compared to those, the proposed method allows assessment of the contribution of building modules in bacterial cells. The dynamic range may be further improved by the use of an alternative bimolecular reconstitution molecule with decreased intrinsic affinity and a lower background in bacteria.²⁹

Additionally, the degree of change observed in *in vivo* fluorescence between different designs most likely depends not only on the building block under investigation but on the type and position of other CC building blocks constituting the assembly (in the case of TRI6, pairs P3S:P4S and P7S:P8S). To account for this, the same scaffold could be used for evaluation of the applicability of novel CC building blocks for the design of CCPO cages.

CONCLUSION

In conclusion, we have designed a polypeptide that self-assembles into a nanoscale triangle *in vivo*. A triangle represents the smallest framework for prototyping building modules to screen natural or designed building modules. The SAXS scattering curve of the polypeptide triangle TRI6 and the helical content match the predicted molecular model.

The resulting polypeptide design was implemented as a platform for detecting folding directly in bacterial cells. This demonstrates the ability of the method to detect polypeptides with coinciding N- and C-termini. We expect that the proposed method will be useful for high throughput screening of designs for single-chain polypeptide polyhedra and possibly other folds from concatenated coiled-coil polypeptides. In addition to being a simple prototyping unit, triangles also represent the convenient fundamental building unit since their geometry is uniquely defined just by the length of the three edges without having to define the angles. Triangles could be used as building blocks for larger assemblies by the introduction of interaction domains into their vertices. Since the number of available orthogonal CC modules is much smaller than the number of nucleic acid building blocks, the strategy of using triangles could be an advantage as the same CC-dimer building blocks could be used in different building modules. Alternatively, assemblies using triangles could be formed through their edges, where four helical bundles would result from assembling CC dimers.³⁰

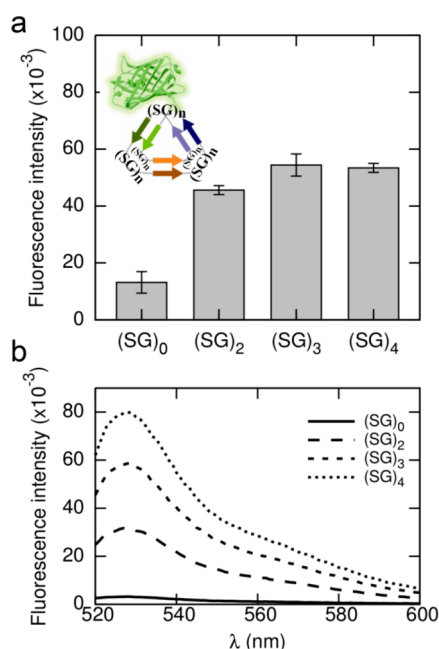


Figure 4. Effect of the linker length ((SG)_n; n = 0, 2, 3, 4) on the reconstitution of the split fluorescent protein in a polypeptide triangle. (a) Relative fluorescence intensity of bacterial cell suspensions expressing TRI6-(SG)₀^{split-mVenus}, TRI6-(SG)₂^{split-mVenus}, TRI6-(SG)₃^{split-mVenus}, and TRI6-(SG)₄^{split-mVenus}. Data are the means of three independent samples. (b) Relative fluorescence intensity of the purified polypeptides TRI6-(SG)₀^{split-mVenus}, TRI6-(SG)₂^{split-mVenus}, TRI6-(SG)₃^{split-mVenus}, and TRI6-(SG)₄^{split-mVenus}.

MATERIALS AND METHODS

Detailed experimental methods are available in the [Supporting Information](#).

ASSOCIATED CONTENT

Supporting Information

The Supporting Information is available free of charge at <https://pubs.acs.org/doi/10.1021/acscchembio.0c00812>.

Detailed methods; descriptions for all materials and measurements; amino acid sequences of all coiled coil-forming peptide segments and polypeptides used in this study; extended biochemical data from polypeptide characterization by SDS-PAGE, SEC-MALS, and SAXS; schematic representation of protein fusions ([PDF](#))

AUTHOR INFORMATION

Corresponding Author

Roman Jerala – Department of Synthetic Biology and Immunology, National Institute of Chemistry, 1000 Ljubljana, Slovenia; EN-FIST Centre of Excellence, 1000 Ljubljana, Slovenia; orcid.org/0000-0001-8024-8871; Email: roman.jerala@KI.si

Authors

Sabina Božič Abram – Department of Synthetic Biology and Immunology, National Institute of Chemistry, 1000 Ljubljana, Slovenia

Helena Gradišar – Department of Synthetic Biology and Immunology, National Institute of Chemistry, 1000 Ljubljana, Slovenia; EN-FIST Centre of Excellence, 1000 Ljubljana, Slovenia

Jana Aupič – Department of Synthetic Biology and Immunology, National Institute of Chemistry, 1000 Ljubljana, Slovenia

Adam R. Round – EMBL Grenoble outstation, 38042 Grenoble, France; School of Chemical and Physical Sciences, Keele University, Keele, Staffordshire, United Kingdom

Complete contact information is available at:

<https://pubs.acs.org/doi/10.1021/acscchembio.0c00812>

Author Contributions

S.B.A., H.G., J.A., and R.J. designed the CCPO triangle-forming variants, ran the experiments, and discussed the results. J.A. and A.R.R. performed the SAXS experiments and SAXS data analysis. S.B.A. and H.G. did other experimental work. R.J. and H.G. conceived the study. The manuscript was written by R.J. and H.G. with contributions of S.B.A. and J.A. All authors have given approval to the final version of the manuscript.

Author Contributions

[†]These authors contributed equally.

Notes

The authors declare no competing financial interest.

ACKNOWLEDGMENTS

This project was financed by Slovenian Research Agency (program no. P4-0176, project N4-0037), a grant from the ICGEB (CRP/SLO14-03) and by the ERANET SynBio project Bioorigami (ERASYNBIO1-006). Support of COST actions CM-1306 and CM-1304 is acknowledged. The synchrotron SAXS data were collected at beamline BM29 at

the European Synchrotron Radiation Facility (ESRF), Grenoble, France.

ABBREVIATIONS

CC, coiled coil; CCPO, coiled-coil protein origami; PmS, PnS, orthogonal heterodimeric coiled-coil-forming pair; TRI6, triangle-forming sequence composed of six concatenated designed modules; CD, circular dichroism; SEC-MALS, size-exclusion chromatography coupled with multiangle light scattering; SAXS, small-angle X-ray scattering; PBS, phosphate buffered saline

REFERENCES

- (1) Rothmund, P. W. (2006) Folding DNA to Create Nanoscale Shapes and Patterns. *Nature* 440, 297–302.
- (2) Seeman, N. C. (2010) Nanomaterials Based on DNA. *Annu. Rev. Biochem.* 79, 65–87.
- (3) Kočar, V., Schreck, J. S., Čeru, S., Gradišar, H., Basić, N., Pisanski, T., Doye, J. P., and Jerala, R. (2016) Design Principles for Rapid Folding of Knotted DNA Nanostructures. *Nat. Commun.* 7, 10803–10810.
- (4) Zhou, W., Šmidlehner, T., and Jerala, R. (2020) Synthetic Biology Principles for the Design of Protein with Novel Structures and Functions. *FEBS Lett.* 594, 2199–2212.
- (5) Azuma, Y., Zschoche, R., Tinzl, M., and Hilvert, D. (2016) Quantitative Packaging of Active Enzymes into a Protein Cage. *Angew. Chem., Int. Ed.* 55, 1531–1534.
- (6) Worsdorfer, B., Woycechowsky, K. J., and Hilvert, D. (2011) Directed Evolution of a Protein Container. *Science* 331, 589–592.
- (7) King, N. P., Sheffler, W., Sawaya, M. R., Vollmar, B. S., Sumida, J. P., Andre, I., Gonen, T., Yeates, T. O., and Baker, D. (2012) Computational Design of Self-Assembling Protein Nanomaterials with Atomic Level Accuracy. *Science* 336, 1171–1174.
- (8) King, N. P., Bale, J. B., Sheffler, W., McNamara, D. E., Gonen, S., Gonen, T., Yeates, T. O., and Baker, D. (2014) Accurate Design of Co-Assembling Multi-Component Protein Nanomaterials. *Nature* 510, 103–108.
- (9) Bale, J. B., Gonen, S., Liu, Y., Sheffler, W., Ellis, D., Thomas, C., Cascio, D., Yeates, T. O., Gonen, T., King, N. P., and Baker, D. (2016) Accurate Design of Megadalton-Scale Two-Component Icosahedral Protein Complexes. *Science* 353, 389–394.
- (10) Padilla, J. E., Colovos, C., and Yeates, T. O. (2001) Nanohedra: Using Symmetry to Design Self Assembling Protein Cages, Layers, Crystals, and Filaments. *Proc. Natl. Acad. Sci. U. S. A.* 98, 2217–2221.
- (11) Sinclair, J. C., Davies, K. M., Venien-Bryan, C., and Noble, M. E. (2011) Generation of Protein Lattices by Fusing Proteins with Matching Rotational Symmetry. *Nat. Nanotechnol.* 6, 558–562.
- (12) Badiyean, S., Sciore, A., Eschweiler, J. D., Koldewey, P., Cristie-David, A. S., Ruotolo, B. T., Bardwell, J. C. A., Su, M., and Marsh, E. N. G. (2017) Symmetry-Directed Self-Assembly of a Tetrahedral Protein Cage Mediated by de Novo-Designed Coiled Coils. *ChemBioChem* 18, 1888–1892.
- (13) Cristie-David, A. S., Chen, J., Nowak, D. B., Bondy, A. L., Sun, K., Park, S. I., Banaszak Holl, M. M., Su, M., and Marsh, E. N. G. (2019) Coiled-Coil-Mediated Assembly of an Icosahedral Protein Cage with Extremely High Thermal and Chemical Stability. *J. Am. Chem. Soc.* 141, 9207–9216.
- (14) Fletcher, J. M., Harniman, R. L., Barnes, F. R. H., Boyle, A. L., Collins, A., Mantell, J., Sharp, T. H., Antognozzi, M., Booth, P. J., Linden, N., Miles, M. J., Sessions, R. B., Verkade, P., and Woolfson, D. N. (2013) Self-Assembling Cages from Coiled-Coil Peptide Modules. *Science* 340, 595–599.
- (15) Kobayashi, N., Yanase, K., Sato, T., Unzai, S., Hecht, M. H., and Arai, R. (2015) Self-Assembling Nano-Architectures Created from a Protein Nano-Building Block Using an Intermolecularly Folded Dimeric de Novo Protein. *J. Am. Chem. Soc.* 137, 11285–11293.

- (16) Ross, J. F., Bridges, A., Fletcher, J. M., Shoemark, D., Alibhai, D., Bray, H. E. V., Beesley, J. L., Dawson, W. M., Hodgson, L. R., Mantell, J., Verkade, P., Edge, C. M., Sessions, R. B., Tew, D., and Woolfson, D. N. (2017) Decorating Self-Assembled Peptide Cages with Proteins. *ACS Nano* 11, 7901–7914.
- (17) Bai, W., Sargent, C. J., Choi, J. M., Pappu, R. V., and Zhang, F. (2019) Covalently-Assembled Single-Chain Protein Nanostructures with Ultra-High Stability. *Nat. Commun.* 10, 3317–3326.
- (18) Lapenta, F., Aupič, J., Strmšek, Ž., and Jerala, R. (2018) Coiled Coil Protein Origami: From Modular Design Principles towards Biotechnological Applications. *Chem. Soc. Rev.* 47, 3530–3542.
- (19) Woolfson, D. N. (2005) The design of Coiled-Coil Structures and Assemblies. *Adv. Protein Chem.* 70, 79–112.
- (20) Drobnak, I., Gradišar, H., Ljubetič, A., Merljak, E., and Jerala, R. (2017) Modulation of Coiled-Coil Dimer Stability through Surface Residues While Preserving Pairing Specificity. *J. Am. Chem. Soc.* 139, 8229–8236.
- (21) Boyle, A. L., Bromley, E. H., Bartlett, G. J., Sessions, R. B., Sharp, T. H., Williams, C. L., Curmi, P. M., Forde, N. R., Linke, H., and Woolfson, D. N. (2012) Squaring the Circle in Peptide Assembly: From Fibers to Discrete Nanostructures by de Novo Design. *J. Am. Chem. Soc.* 134, 15457–15467.
- (22) Noble, J. E., De Santis, E., Ravi, J., Lamarre, B., Castelletto, V., Mantell, J., Ray, S., and Ryadnov, M. G. A. (2016) De Novo Virus-Like Topology for Synthetic Virions. *J. Am. Chem. Soc.* 138, 12202–12210.
- (23) Gradišar, H., Božič, S., Doles, T., Vengust, D., Hafner-Bratkovič, I., Mertelj, A., Webb, B., Sali, A., Klavžar, S., and Jerala, R. (2013) Design of a Single-Chain Polypeptide Tetrahedron Assembled from Coiled-Coil Segments. *Nat. Chem. Biol.* 9, 362–366.
- (24) Ljubetič, A., Lapenta, F., Gradišar, H., Drobnak, I., Aupič, J., Strmšek, Ž., Lainšček, D., Hafner-Bratkovič, I., Majerle, A., Krivec, N., Benčina, M., Pisanski, T., Veličković, T. Č., Round, A., Carazo, J. M., Melero, R., and Jerala, R. (2017) Design of Coiled-Coil Protein-Origami Cages That Self-Assemble in Vitro and in Vivo. *Nat. Biotechnol.* 35, 1094–1101.
- (25) Gradišar, H., and Jerala, R. (2011) De Novo Design of Orthogonal Peptide Pairs Forming Parallel Coiled-Coil Heterodimers. *J. Pept. Sci.* 17, 100–106.
- (26) Ljubetič, A., Drobnak, I., Gradišar, H., and Jerala, R. (2016) Designing the Structure and Folding Pathway of Modular Topological Bionanostructures. *Chem. Commun.* 52, 5220–5229.
- (27) Park, W. M., Bedewy, M., Berggren, K. K., and Keating, A. E. (2017) Modular Assembly of a Protein Nanotriangle Using Orthogonally Interacting Coiled Coils. *Sci. Rep.* 7, 10577–10586.
- (28) He, Y., Ye, T., Su, M., Zhang, C., Ribbe, A. E., Jiang, W., and Mao, C. D. (2008) Hierarchical Self-Assembly of DNA into Symmetric Supramolecular Polyhedra. *Nature* 452, 198–201.
- (29) Zaccai, N. R., Chi, B., Thomson, A. R., Boyle, A. L., Bartlett, G. J., Bruning, M., Linden, N., Sessions, R. B., Booth, P. J., Brady, R. L., and Woolfson, D. N. (2011) A de Novo Peptide Hexamer with a Mutable Channel. *Nat. Chem. Biol.* 7, 935–941.
- (30) Chen, Z., Boyken, S. E., Jia, M., Busch, F., Flores-Solis, D., Bick, M. J., Lu, P., VanAernum, Z. L., Sahasrabudde, A., Langan, R. A., Bermeo, S., Brunette, T. J., Mulligan, V. K., Carter, L. P., DiMaio, F., Sgourakis, N. G., Wysocki, V. H., and Baker, D. (2019) Programmable Design of Orthogonal Protein Heterodimers. *Nature* 565, 106–111.